Interaction of phospholipid scramblase 1 with the Epstein-Barr virus protein BZLF1 represses BZLF1-mediated lytic gene transcription

Received for publication, March 1, 2019, and in revised form, August 15, 2019 Published, Papers in Press, August 21, 2019, DOI 10.1074/jbc.RA119.008193

Shuichi Kusano[1] **and Masanori Ikeda**

From the Division of Biological Information Technology, Joint Research Center for Human Retrovirus Infection, Kagoshima University, 8-35-1 Sakuragaoka, Kagoshima-shi, Kagoshima 890-8544, Japan

Edited by Charles E. Samuel

Human phospholipid scramblase 1 (PLSCR1) is strongly expressed in response to interferon (IFN) treatment and viral infection, and PLSCR1 has been suggested to play an important role in IFN-dependent antiviral responses. In this study, we showed that the basal expression of PLSCR1 was significantly elevated in Epstein-Barr virus (EBV)–infected nasopharyngeal carcinoma (NPC). PLSCR1 was observed to directly interact with the EBV immediate-early transactivator BZLF1 *in vitro* and *in vivo*, and this interaction repressed the BZLF1-mediated transactivation of an EBV lytic BMRF1 promoter construct. In addition, PLSCR1 expression decreased the BZLF1-mediated up-regulation of lytic BMRF1 mRNA and protein expression in WT and PLSCR1-knockout EBV-infected NPC cells. Furthermore, we showed that PLSCR1 represses the interaction between BZLF1 and CREB-binding protein (CBP), which enhances the BZLF1-mediated transactivation of EBV lytic promoters. These results reveal for the first time that PLSCR1 specifically interacts with BZLF1 and negatively regulates its transcriptional regulatory activity by preventing the formation of the BZLF1-CBP complex. This interaction may contribute to the establishment of latent EBV infection in EBV-infected NPC cells.

Epstein-Barr virus (EBV)[2] is linked to the development of several malignancies, including endemic Burkitt's lymphoma (BL), posttransplantation lymphoma, Hodgkin's disease, nasopharyngeal carcinoma (NPC), and some types of gastric cancers (1, 2). EBV can cause both latent and lytic infections, typically establishing latent infections in B cells and lytic infections in epithelial cells (3–5). However, the latent form of EBV can be detected in EBV-associated malignancies of both lymphoid and epithelial origin (3–5). B cell–specific transcription factors have been reported to promote the latent EBV infection of B cells by directly interacting with and inhibiting the function of BZLF1 (also termed Z, Zta, or ZEBRA), an EBV-encoded immediate-early lytic gene product (6, 7). The establishment of latent infections and/or the inhibition of lytic infections may play an important role in the development of EBV-associated epithelial malignancies. However, the specific cellular factors required for the negative regulation of lytic infections in EBV-associated epithelial malignancies remain poorly understood.

BZLF1 plays a crucial role in the switch from latent to lytic EBV infections (8, 9). BZLF1 contains an N-terminal transactivation domain and a C-terminal basic leucine zipper (bZIP) motif. As a bZIP transcription factor that is homologous to c-Jun and c-Fos, BZLF1 binds as a homodimer to consensus AP-1 sites and AP-1–like motifs known as BZLF1-responsive elements (10, 11). The binding of BZLF1 to BZLF1-responsive elements and AP-1 sites results in the transactivation of viral and specific cellular promoters, leading to an ordered cascade of viral gene expression in which the expression of early genes involved in DNA replication and metabolism is followed by that of late genes encoding viral structural proteins (8, 11).

Human phospholipid scramblase 1 (PLSCR1) was identified as an enzyme involved in the calcium-dependent, nonspecific, rapid redistribution of phospholipids (12). However, further studies have suggested that PLSCR1 is not involved in phospholipid redistribution when a perturbation of plasma membrane asymmetry is required following cell activation or apoptosis (13, 14). Furthermore, the results of recent studies suggest that PLSCR1 inhibits tumorigenesis, promotes apoptosis, and facilitates the differentiation of myeloid cells through its interaction with several signaling molecules (15, 16). Human PLSCR1 expression is robustly induced in response to IFN treatment and viral infection (17–19). In addition, PLSCR1 has been reported to enhance the IFN-dependent induction of IFN-stimulated gene expression and antiviral activity, and PLSCR1 has been suggested to play an important role in IFN-dependent antiviral responses (18). However, PLSCR1 is not involved in the IFN-α-mediated induction of IFN-stimulated gene 15 expression in our CRISPR/Cas9-generated PLSCR1-KO HEK-293 cells (Fig. S1), and the precise mechanisms of PLSCR1-mediated antiviral activity remain unclear. Recently, we and other groups reported that PLSCR1 directly interacts with and

This work was supported by Japan Society for the Promotion of Science (JSPS) Grant JP19K07644 (to S. K.) and by A Grant from Kodama Memorial Fund for Medical Research (to S. K.). The authors declare that they have no conflicts of interest with the contents of this article.
This article contains Figs. S1–S3.

[1] To whom correspondence should be addressed: Tel.: 81-99-275-5936; Fax.: 81-275-5937; E-mail: k2873052@kadai.jp.

[2] The abbreviations used are: EBV, Epstein-Barr virus; 3FG, 3×FLAG epitope; 3M, 3×myc epitope; BL, Burkitt's lymphoma, bZIP, basic leucine zipper; CBP, CREB-binding protein; CREB, cAMP-response element-binding protein; G3PDH, glyceraldehyde-3-phosphate dehydrogenase; HTLV, human T-cell leukemia virus; ID, intrinsically disordered; NPC, nasopharyngeal carcinoma; PLSCR1, phospholipid scramblase 1; PS, penicillin and streptomycin; IFN, interferon; KO, knockout.

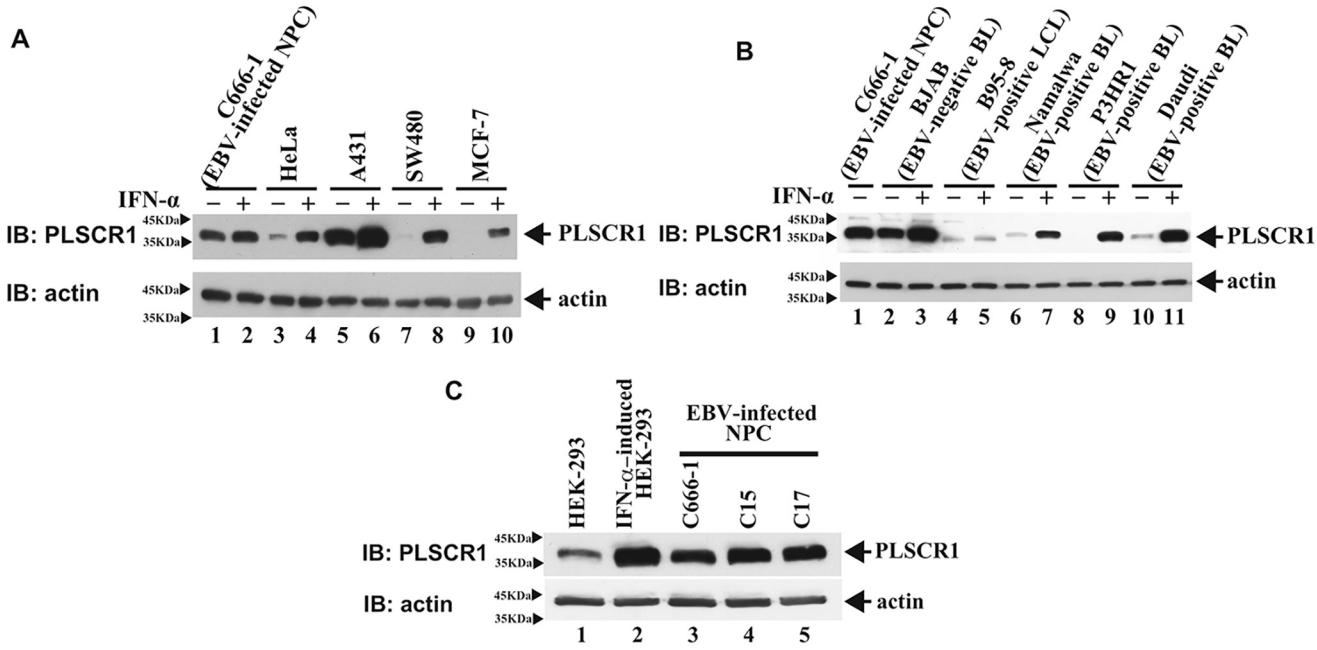

Figure 1. PLSCR1 expression is highly induced in EBV-infected NPC cells in the absence of IFN-α-2b treatment. *A–C*, cells were treated with or without 3000 units/ml of IFN-α-2b for 16 h. Total cell lysates were prepared using RIPA buffer (Sigma), and a total of 15 μg (*A*), 8 μg (*B*), or 10 μg (*C*) of total cell lysates were subjected to SDS-PAGE. Immunoblotting (*IB*) was performed using an anti-PLSCR1 antibody for endogenous PLSCR1 or an anti-actin antibody for endogenous actin. *LCL*, lymphoblastoid cell line.

affects the function of several viral proteins (20–23), which may be important for PLSCR1-mediated antiviral activity.

In this study, we showed that the basal expression of PLSCR1 is significantly elevated in EBV-infected NPC cells. PLSCR1 directly and specifically interacts with the bZIP motif of BZLF1 through its 1–163 and 160–250 amino acid regions. PLSCR1 overexpression was observed to repress the BZLF1-mediated transactivation of an EBV early BMRF1 promoter reporter construct in an interaction-dependent manner. In addition, PLSCR1 overexpression decreased the BZLF1-mediated expression of lytic BMRF1 at the mRNA and protein levels in the WT and PLSCR1-KO EBV-infected NPC cell line C666-1. Furthermore, PLSCR1 was observed to repress the interaction between BZLF1 and the transcriptional co-activator CREB-binding protein (CBP), which is required for the efficient transactivation of EBV early promoters by BZLF1.

These results reveal for the first time that PLSCR1 specifically interacts with BZLF1 and negatively regulates its transcriptional regulatory activity by preventing its interaction with CBP. This interaction may contribute to the establishment of latent EBV infection in EBV-infected NPC cells.

Results

Basal PLSCR1 expression is significantly elevated in EBV-infected NPC cells

Human PLSCR1 expression has been shown to be induced in response to IFN treatment and viral infection (17, 18). The expression of PLSCR1 was determined in the presence and absence of IFN treatment in the EBV-infected NPC cell line C666-1 and in EBV-negative epithelial cells. The basal expression of PLSCR1 was significantly lower in HeLa, SW480, and MCF-7 cells in the absence of IFN treatment. However, PLSCR1 expression was significantly induced in these cell lines in the presence of IFN-α-2b (Fig. 1*A*, *lanes 3*, *4*, and *7–10*), consistent with our previous report (21). Interestingly, the basal expression of PLSCR1 was robustly higher in C666-1 and A431 cells in the absence of IFN treatment (Fig. 1*A*, *lanes 1* and *5*). In addition, the expression of PLSCR1 was weakly induced by the IFN treatment in these cell lines (Fig. 1*A*, *lanes 1, 2, 5,* and *6*).

Next, to assess whether the basal expression of PLSCR1 was also increased in EBV-infected B cells, we evaluated PLSCR1 expression in EBV-negative and EBV-positive B cell lines. Consistent with previous observations of other lymphoid cells (21, 24), the basal expression of PLSCR1 in EBV-negative Burkitt's lymphoma BJAB cells was markedly high, similar to that observed in the C666-1 cells, in the absence of IFN. In contrast with the results obtained in C666-1 cells, PLSCR1 expression was significantly induced by the IFN treatment in BJAB cells (Fig. 1*B*, *lanes 1–3*). Notably, PLSCR1 expression was difficult to detect in all EBV-positive B cell lines tested in the absence of IFN treatment. However, PLSCR1 expression was significantly induced by the IFN treatment, except in B95–8 cells (Fig. 1*B*, *lanes 4–11*). Although B95–8 cells originate from marmoset B cells, the sequences of human PLSCR1 and marmoset PLSCR1 are highly homologous, with 90% identity and 95% similarity, and marmoset PLSCR1 is likely to be detected by the anti-human PLSCR1 polyclonal antibody. However, human IFN-α-2b may be ineffective at inducing IFN signaling in marmoset B cells.

To confirm whether PLSCR1 expression was also induced in other EBV-infected epithelial cells, we analyzed the basal PLSCR1 levels in EBV-infected NPC xenograft C15 and C17 tumors. The basal expression levels of PLSCR1 were signifi-

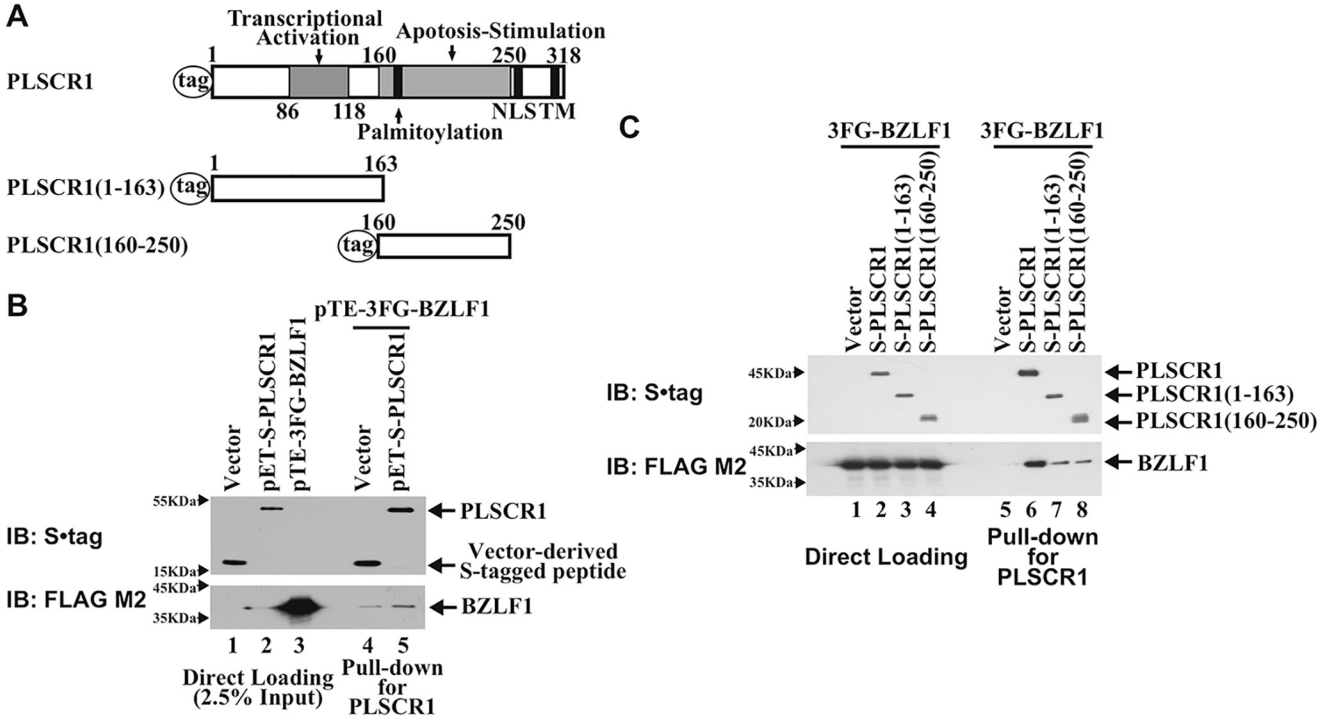

Figure 2. PLSCR1 directly interacts with BZLF1 through amino acids 1–163 and 160–250. *A*, schematic representation of PLSCR1 and its truncated mutant expression constructs containing epitope tags at the N termini. The PLSCR1 structural motifs have been described previously (21) and annotated as follows: Palmitoylation, palmitoylation sites; *NLS*, nuclear localization signal; *TM*, transmembrane domain. *B*, bacterial lysates prepared in CHAPS lysis buffer were mixed and incubated with S-protein beads to precipitate PLSCR1 as follows: 100 μg of pET32a(+) vector or pET-S-PLSCR1 lysate and 30 μg of pTE-3FG-BZLF1 lysate were used. Following pulldowns, 0.8 μg of total bacterial lysates and the precipitated complexes were divided into two portions and subjected to SDS-PAGE. Immunoblotting was performed using an anti–S-tag antibody for PLSCR1 or an anti-FLAG M2 antibody for BZLF1. *C*, HEK-293 cells were transfected with 1 μg of pcDNA3 or 3FG-BZLF1 and 2 μg of pcDNA3, 0.7 μg of S-PLSCR1, 2 μg of S-PLSCR1(1–163) or 2 μg of S-PLSCR1(160–250). The total amount transfected was equalized by adding pcDNA3. A total of 400 μg of total cell lysate prepared in CHAPS lysis buffer was incubated with S-protein beads to precipitate PLSCR1 and its mutants. Following pulldowns, 20 μg of total cell lysate and the precipitated complexes were divided into two portions and subjected to SDS-PAGE. Immunoblotting was performed using an anti-FLAG M2 antibody for BZLF1 or an S-tag antibody for PLSCR1 and its mutants.

cantly decreased in HEK-293 cells (Fig. 1*C*, *lane 1*), consistent with previous observations (21). However, the basal expression levels of PLSCR1 were significantly increased in EBV-infected NPC xenograft C15 and C17 tumors, similar to those in C666-1 and IFN-α–induced HEK-293 cells (Fig. 1*C*, *lanes 2–5*). These observations indicated that the basal expression of PLSCR1 was significantly elevated in all EBV-infected NPC cells tested.

PLSCR1 directly interacts with the EBV lytic transactivator BZLF1

PLSCR1 has been reported to repress the functions of viral transactivators, including the human T-cell leukemia virus (HTLV)-1 Tax, HIV-1 Tat, and human hepatitis B virus HBx proteins, through direct interaction (21, 22, 25). It is possible that PLSCR1 also interacts with and negatively regulates the EBV-encoding transactivator BZLF1, which stimulates the transcription of genes that causes the switch from latent to lytic EBV infection. To determine whether PLSCR1 directly interacts with BZLF1, full-length PLSCR1 encoding amino acids 1–318 was tagged with the trxA and S epitopes (pET-S-PLSCR1) (Fig. 2*A*), and a BZLF1 truncation encoding amino acids 3–245 was tagged with a 3×FLAG epitope (pTE-3FG-BZLF1) (Fig. 3*A*). These constructs were expressed in *Escherichia coli*, after which the bacterial cell lysates were mixed, and pulldown assays were performed using S-protein beads to precipitate PLSCR1. Immunoblot analyses of the PLSCR1-containing complexes revealed that BZLF1 was efficiently co-precipitated with PLSCR1 (Fig. 2*B*, *lane 5*), whereas the empty vector-transformed lysates precipitated only trace amounts of PLSCR1 (Fig. 2*B*, *lane 4*). These results indicated that PLSCR1 directly interacts with BZLF1 *in vitro*.

PLSCR1 contains several functional domains, including three predicted intrinsically disordered (ID) regions (21) and the N-terminal– and central ID region–containing domains involved in interacting with target proteins (21, 22, 26). To identify which PLSCR1 regions are involved in this interaction *in vivo*, S epitope–tagged full-length PLSCR1 (S-PLSCR1) or its truncated mutants encoding amino acids 1–163 (S-PLSCR1(1–163)) or 160–250 (S-PLSCR1(160–250)) were expressed in HEK-293 cells together with a 3×FLAG epitope–tagged BZLF1 encoding amino acids 3–245 (3FG-BZLF1). Immunoblot analysis of the total cell lysates indicated that all constructs were expressed at similar levels (Fig. 2*C*, *lanes 2–4*). However, immunoblot analysis of the complexes containing PLSCR1 or its truncated mutants revealed that BZLF1 was efficiently co-precipitated with PLSCR1 (Fig. 2*C*, *lane 6*) but weakly co-precipitated with PLSCR1(1–163) and PLSCR1(160–250) (Fig. 2*C*, *lanes 7* and *8*). These observations revealed that PLSCR1 contains two BZLF1-binding regions and that the amino acid regions 1–163 and 160–250 of PLSCR1 are sufficient for this interaction.

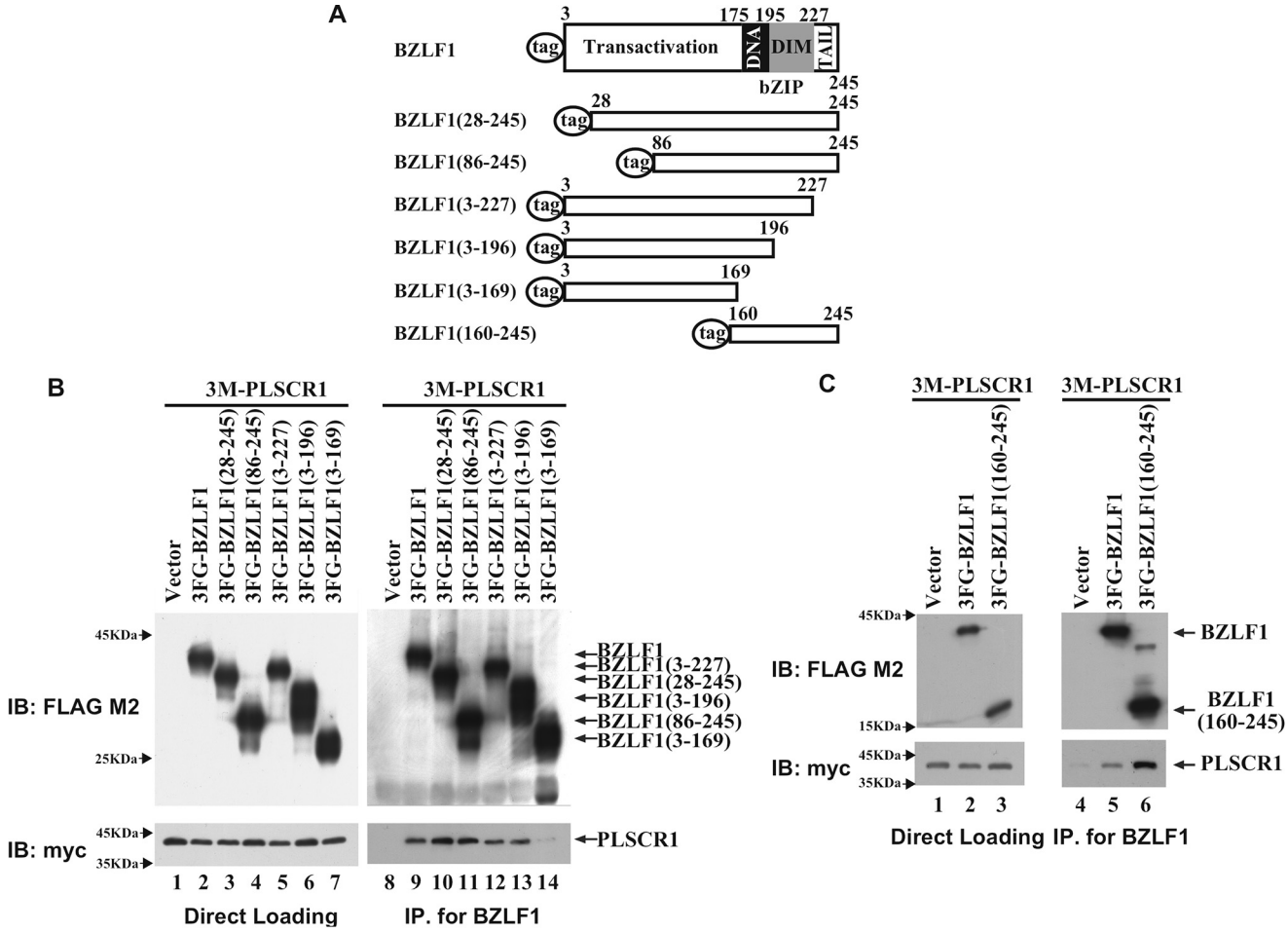

Figure 3. bZIP motif of BZLF1 is sufficient for its interaction with PLSCR1. *A*, schematic representation of BZLF1 and its truncated mutant expression constructs containing epitope tags at the N termini. The structural motifs of BZLF1 are annotated as follows: Transactivation, transactivation domain; bZIP, basic leucine zipper motif; DNA, DNA-binding domain; DIM, dimerization domain; and TAIL, C-terminal tail (34). *B*, HEK-293 cells were transfected with 3.5 μg of 3M-PLSCR1 and 1.5 μg of pcDNA3, 3FG-BZLF1, 3FG-BZLF1(28–245), 3FG-BZLF1(86–245), 3FG-BZLF1(3–227), 3FG-BZLF1(3–196), or 3FG-BZLF1(3–169). A total of 300 μg of total cell lysate prepared in CHAPS lysis buffer was incubated with anti-FLAG M2 beads to precipitate BZLF1 and its mutants. Following immunoprecipitation, 15 μg of total cell lysate and the precipitated complexes were divided into two portions and subjected to SDS-PAGE. Immunoblotting was performed using an anti-myc antibody for PLSCR1 or an anti-FLAG M2 antibody for BZLF1 and its mutants. *IP*, immunoprecipitation. *C*, HEK-293 cells were transfected with 3.5 μg of 3M-PLSCR1 and 1.5 μg of pcDNA3, 3FG-BZLF1, or 3FG-BZLF1(160–245). A total of 300 μg of total cell lysate prepared in CHAPS lysis buffer was incubated with anti-FLAG M2 beads to precipitate BZLF1 and its mutants. Following immunoprecipitation, 20 μg of total cell lysate and the precipitated complexes were divided into two portions and subjected to SDS-PAGE. Immunoblotting was performed using an anti-myc antibody for PLSCR1 or an anti-FLAG M2 antibody for BZLF1 and mutant.

C-terminal bZIP-containing region of BZLF1 is sufficient for binding to PLSCR1

To identify which region of BZLF1 is required for the interaction with PLSCR1, 3FG-BZLF1 or 3×FLAG epitope–tagged truncated mutants of BZLF1-encoding amino acids 86–245 (3FG-BZLF1(86–245)), 3–227 (3FG-BZLF1(3–227)), 3–196 (3FG-BZLF1(3–196)), or 3–169 (3FG-BZLF1(3–169)) (Fig. 3*A*) were co-expressed in HEK-293 cells with full-length PLSCR1 tagged with three myc epitopes (3M-PLSCR1). Immunoblot analysis of the total cell lysates indicated that all constructs were expressed at similar levels (Fig. 3*B*, *lanes 1–7*). Subsequent immunoblot analysis of the immunoprecipitated full-length or truncated BZLF1 complexes revealed that BZLF1(3–169) did not co-precipitate with PLSCR1 (Fig. 3*B*, *lane 14*), whereas BZLF1, BZLF1(86–245), BZLF1(3–227), and BZLF1(3–196) efficiently co-precipitated with PLSCR1 (Fig. 3*B*, *lanes 9–13*). These findings indicated that amino acids 170–196 of BZLF1, which are included within the DNA-binding domain of the bZIP motif (27), are required for the interaction of BZLF1 with PLSCR1.

To further confirm this interaction, 3FG-BZLF1 and a 3×FLAG epitope–tagged C-terminal bZIP motif of BZLF1 encoding amino acids 160–245 (3FG-BZLF1(160–245)) (Fig. 3*A*) were expressed in HEK-293 cells and assessed for their ability to bind to PLSCR1. Immunoblot analysis of the immunoprecipitated complexes containing BZLF1 or BZLF1 bZip motif revealed that PLSCR1 was co-precipitated with both BZLF1 and BZLF1(160–245) (Fig. 3*C*, *lanes 5* and *6*). These results revealed that the C-terminal bZIP motif–containing region of BZLF1 is sufficient for its interaction with PLSCR1 *in vivo*.

PLSCR1 does not affect the nuclear localization of BZLF1

PLSCR1 is localized at the plasma membrane and in various internal membrane pools. However, PLSCR1 also localizes to

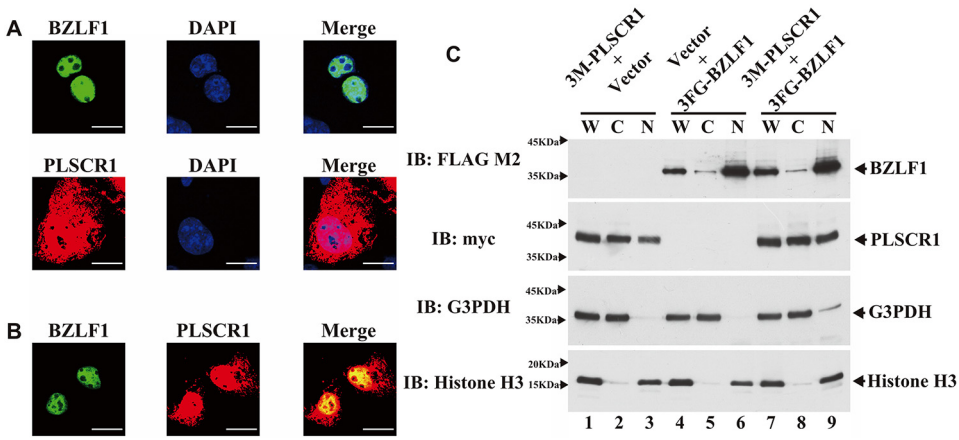

Figure 4. PLSCR1 and BZLF1 co-localize in the nucleus. *A*, COS-1 cells were transfected with 50 ng of 3FG-BZLF1 or 3M-PLSCR1. The cells were stained using an anti-FLAG M2 antibody to identify BZLF1 (*green*) or an anti-myc antibody to identify PLSCR1 (*red*). The cell nuclei were stained with DAPI. DAPI- and FLAG M2– or myc-stained images were acquired using an FV500 confocal laser scanning microscope (Olympus) and merged using FLUOVIEW (Olympus). *Scale bar*, 20 μm. *B*, COS-1 cells were transfected with 50 ng of 3FG-BZLF1 and 150 ng of 3M-PLSCR1. The cells were stained in the same manner as described for *panel A*. FLAG M2– and myc-stained fluorescence images were acquired using a FV500 CLSM instrument and merged using FLUOVIEW. *Yellow* areas indicate the co-localization of the two proteins. *Scale bar*, 20 μm. *C*, HeLa-PLSKO cells were transfected with 150 ng of 3FG-BZLF1 and/or 2 μg of 3M-PLSCR1. The total amount of plasmid transfected was equalized by adding pcDNA3. Whole cell extractions and subcellular fractionations were performed as described in "Experimental procedures." Then, 5 μg of the whole cell lysate and the cytoplasmic and nuclear fractions were subjected to SDS-PAGE. Immunoblotting (*IB*) was performed with an anti–FLAG M2 antibody for BZLF1, an anti-myc antibody for PLSCR1, an anti-G3PDH antibody for G3PDH (as a cytoplasmic marker) and an anti-histone H3 antibody for histone H3 (as a nucleus marker). *W*, whole cell lysate; *C*, cytoplasmic fraction; *N*, nuclear fraction.

the nucleus in response to cytokine stimulation (28), and BZLF1 has been reported to be primarily localized in the nucleus (29). To further investigate the functional relevance of PLSCR1-BZLF1 complex formation, the intracellular localization of BZLF1 and PLSCR1 was assessed through immunofluorescence analysis. Consistent with previous observations, BZLF1 was primarily detected when PLSCR1 was absent (Fig. 4*A*, *top panel*), whereas PLSCR1 was detected throughout the cytoplasm and nucleus (Fig. 4*A*, *bottom panel*) (21, 22). This nuclear localization pattern of BZLF1 was not affected by the presence of PLSCR1 (Fig. 4*B*).

To confirm this nuclear co-localization of BZLF1 and PLSCR1 using subcellular fractionation, we expressed 3FG-BZLF1 and 3M-PLSCR1 in PLSCR1-KO HeLa (HeLa-PLSKO) cells. Immunoblotting of the whole cell lysates and the cytoplasmic and nuclear fractions indicated that the glyceraldehyde-3-phosphate dehydrogenase (G3PDH) and histone H3 were barely detected in the nuclear and cytoplasmic fractions, respectively, which demonstrated the accuracy of the fractionation (Fig. 4*C*, *third panel from the top* and *bottom panel*). PLSCR1 was efficiently detected in the cytoplasmic and nuclear fractions, and the levels of PLSCR1 in the cytoplasmic fraction were slightly higher than levels in the nuclear fraction in the absence and presence of BZLF1 (Fig. 4*C*, *lanes 1–3* and *7–9*, *second panel from top*). In the absence of PLSCR1, most BZLF1 was localized in the nuclear fraction, and this nuclear localization of BZLF1 was not affected by the expression of PLSCR1 (Fig. 4*C*, *lanes 4–6* and *7–9*, *top panel*). These data confirmed that this interaction does not affect the nuclear localization of BZLF1 and that PLSCR1 and BZLF1 co-localize in the nucleus *in vivo*.

PLSCR1 represses BZLF1-mediated transactivation in an interaction-dependent manner

BZLF1 binds as a homodimer to target DNA through its C-terminal bZIP motif, which interacts with PLSCR1. To determine whether PLSCR1 affects BZLF1-mediated transactivation of early gene promoters, we measured the activity of a luciferase-reporter plasmid under the control of the lytic BMRF1 promoter (pBMRF1pro-4.10) in the presence of 3FG-BZLF1 and S-PLSCR1 in COS-1 cells. In the presence of BZLF1, luciferase activity was increased ~18-fold in the absence of PLSCR1 expression (Fig. 5*A*, *lane 5*). Although PLSCR1 slightly decreased the luciferase activity in the absence of BZLF1, PLSCR1 overexpression efficiently decreased this BZLF1-induced luciferase activity in a dose-dependent manner (Fig. 5*A*, *lanes 6–8*).

To determine whether the binding of PLSCR1 to BZLF1 is sufficient for this repression, we measured the luciferase activity of pBMRF1pro-4.10 in COS-1 and HEK-293 cells containing empty vector or 3FG-BZLF1 and either 3M-PLSCR1, 3M-PLSCR1(1–163), or 3M-PLSCR1(160–250). In COS-1 cells, BZLF1 expression increased the luciferase activity ~3-fold compared with that observed in the empty vector–transfected cells (Fig. 5*B*, *lane 2*). PLSCR1 and PLSCR1(1–163) efficiently decreased this BZLF1-induced luciferase activity to near basal levels (Fig. 5*B*, *lanes 3–6*), whereas this activity was reduced to ~60% of that observed in the empty vector–transfected cells in the presence of PLSCR1(160–250), even when an excess amount of BZLF1 was expressed by transfecting four times more DNA (Fig. 5*B*, *lanes 7* and *8*). In HEK-293 cells, BZLF1 expression increased the luciferase activity ~8-fold compared with that observed in the empty vector–transfected cells (Fig. 5*B*, *lane 10*). PLSCR1 efficiently decreased this BZLF1-induced luciferase activity to lower than 45% of that observed in the empty vector–transfected cells (Fig. 5*B*, *lane 12*), whereas this activity was reduced to ~60 and 75% of that observed in the empty vector–transfected cells in the presence of PLSCR1(1–163) and PLSCR1(160–250), respectively, even when an excess amount of BZLF1 was expressed by transfecting four times more DNA (Fig. 5*B*, *lanes 14* and *16*). These obser-

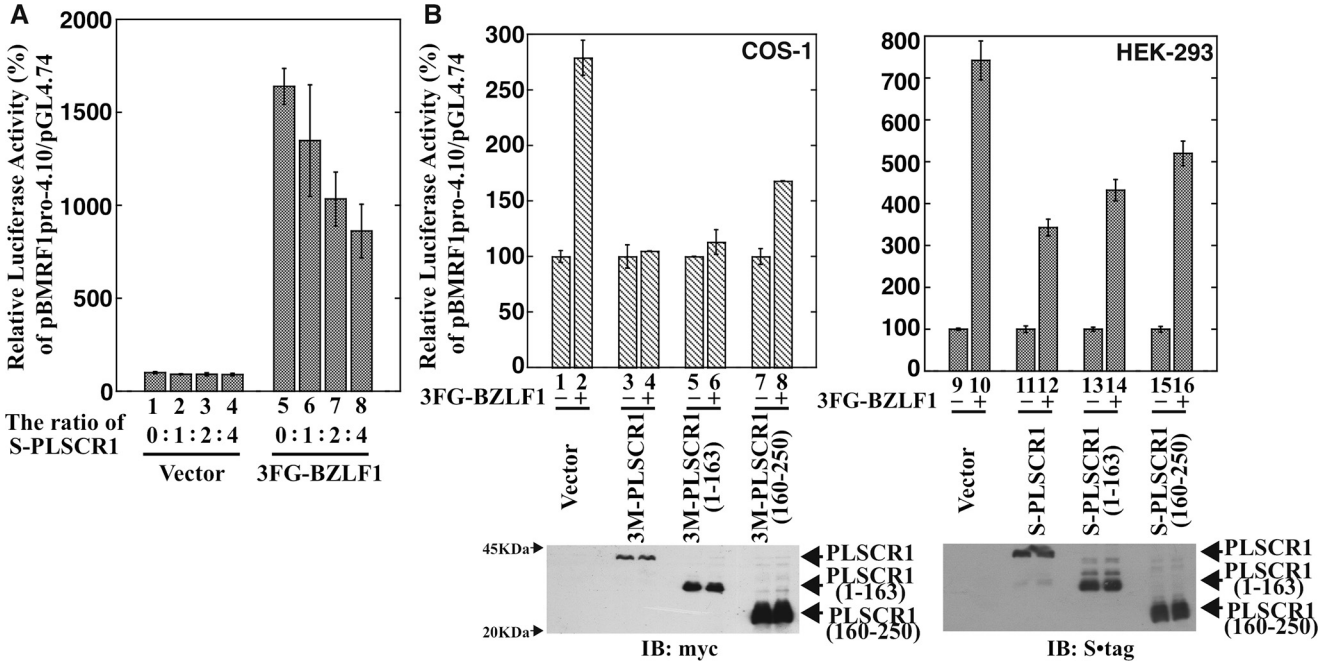

Figure 5. Interaction regions of PLSCR1 are sufficient for the repression of BZLF1-mediated transactivation. *A*, COS-1 cells were transfected with 50 ng of pBMRF1pro-4.10; 25 ng of pGL4.74; 4 ng of 3FG-BZLF1; and 100, 200, or 400 ng of S-PLSCR1 using jetPEI. The total amount of plasmid transfected was equalized by adding pcDNA3. After 24 h of transfection, the cells were lysed and luciferase activities were determined. The firefly luciferase/*Renilla* luciferase activity ratio of cells transfected with the vector only was defined as 100%. The data represent the average relative values from three experiments, and the *error bars* indicate S.D. *B*, COS-1 cells were transfected with 100 ng of pBMRF1pro-4.10; 10 ng of pGL4.74; 2 ng of pcDNA3 or 3FG-BZLF1; and 100 ng of 3M-PLSCR1, 400 ng of 3M-PLSCR1(1–163), or 400 ng of 3M-PLSCR1(160–250) using TransIT-LT1. HEK-293 cells were transfected with 50 ng of pBMRF1pro-4.10; 25 ng of pGL4.74; 1 ng of pcDNA3 or 3FG-BZLF1; and 100 ng of S-PLSCR1, 400 ng of S-PLSCR1(1–163), or 400 ng of S-PLSCR1(160–250). The total amount of plasmid transfected was equalized by adding pcDNA3. After 48 h (COS-1) or 24 h (HEK-293) of transfection, the firefly luciferase and *Renilla* luciferase activities were measured as described for *panel A*. The firefly luciferase/*Renilla* luciferase activity ratio of cells transfected with the PLSCR1 constructs in the presence of the empty vector was defined as 100%. The expression of transfected PLSCR1 and its mutants was monitored by immunoblotting using 1/10 of the volume of the total cell lysates.

vations revealed that the BZLF1-binding regions of PLSCR1 (amino acids 1–163 and 160–250) are sufficient to repress the BZLF1-dependent transactivation of the BMRF1 promoter. However, the N-terminal amino acids 1–163 of PLSCR1, which have been suggested to contain a long ID region, produce a stronger inhibition than amino acids 160–250.

PLSCR1 expression negatively regulates lytic gene expression in EBV-infected NPC cells

To investigate the PLSCR1-mediated repression of BZLF1-dependent transactivation at the endogenous mRNA level in EBV-infected NPC cells, lytic gene expression was induced by transfecting C666-1 cells with 3FG-BZLF1 in the presence and absence of 3M-PLSCR1. Immunoblot analysis of the total cell lysates indicated that all constructs were expressed at similar levels (Fig. 6*A*, *lanes 1–4*, *top panel*). The results of semiquantitative RT-PCR assays demonstrated that the levels of G3PDH mRNA were almost identical in the presence and absence of BZLF1 and PLSCR1 (Fig. 6*A*, *bottom panel*). BMRF1, an early gene in the EBV lytic cycle, was efficiently transcribed in the presence of BZLF1 (Fig. 6*A*, *lane 3*, *third panel from the top*). However, the levels of BMRF1 mRNA were significantly decreased in the presence of PLSCR1 to ~50% of that observed in the empty vector–transfected cells (Fig. 6*A*, *lanes 3* and *4*, *third panel from the top*). These results indicated that PLSCR1 negatively regulates the BZLF1-dependent transactivation of the lytic gene in EBV-infected NPC cells.

Next, we assessed whether a high level of PLSCR1 expression represses endogenous BZLF1-dependent transactivation in EBV-infected NPC cells. PLSCR1 expression was decreased in C666-1 cells transfected with nontarget control or PLSCR1-specific shRNA plasmids (21). In contrast, immunoblot analysis of total cell lysates revealed that PLSCR1 was highly expressed in nontarget shRNA-transfected cells and that PLSCR1-specific shRNA transfection significantly repressed PLSCR1 expression (Fig. 6*B*, *top panel*). The results of semiquantitative RT-PCR assays demonstrated that the levels of G3PDH mRNA in the PLSCR1-specific shRNA-transfected cells were slightly lower than those observed in the nontarget shRNA-transfected cells (Fig. 6*B*, *bottom panel*). However, the levels of BMRF1 mRNA were increased 2.5-fold in the PLSCR1-specific shRNA-transfected cells compared with that observed in the nontarget shRNA-transfected cells (Fig. 6*B*, *third panel from the top*). These results indicated that a high level of PLSCR1 expression represses the BZLF1-dependent transactivation of the lytic genes in EBV-infected NPC cells.

To confirm this PLSCR1-mediated repression of BZLF1-dependent transactivation at the protein level, BMRF1 protein expression was induced in C666-1 cells by transfection with 3FG-BZLF1 in the presence and absence of PLSCR1-specific shRNA transfection. Immunoblot analysis of the total cell lysates indicated that PLSCR1-specific shRNA transfection efficiently decreased endogenous PLSCR1 expression (Fig. 6*C*, *lanes 1–4*, *top panel*) and that the levels of BZLF1 were almost

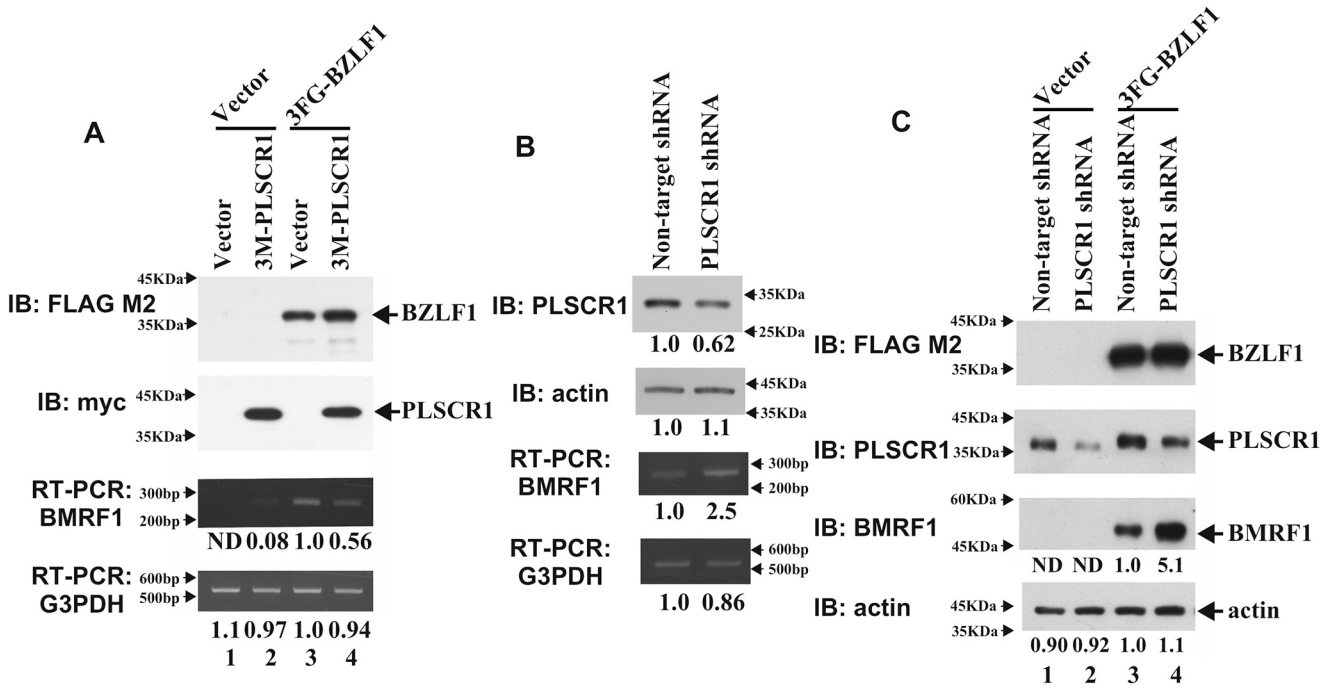

Figure 6. PLSCR1 expression decreases the levels of BMRF1 mRNA and protein in C666-1 cells. *A*, C666-1 cells were transfected with 0.4 μg of pcDNA3 or 3FG-BZLF1 and with 3 μg of pcDNA3 or 3M-PLSCR1. After 48 h of transfection, total cell lysates and total RNA were prepared. Total cell lysates (5 μg) were subjected to SDS-PAGE, and immunoblotting was performed using an anti–FLAG M2 antibody for BZLF1 or an anti-myc antibody for PLSCR1. PCR was performed as follows: 21 cycles of amplification for G3PDH using Hot Start TaqDNA Polymerase (HSTaq) (New England Biolabs) and 23 cycles of amplification for BMRF1 using KAPATaq EXtra HotStart ReadyMix with Dye (KAPATaqEx) (Kapa Biosystems). The intensities of the RT-PCR products were quantified using ImageJ, and the levels of G3PDH or BMRF1 mRNA from the empty vector and 3FG-BZLF1–transfected cells were defined as 1.0. *ND*, not detected. *B*, C666-1 cells were transfected with 3.5 μg of a nontarget shRNA control or PLSCR1-specific shRNA. After 72 h of transfection, total cell lysates and total RNA were prepared. Total cell lysates (8 μg) were subjected to SDS-PAGE, and immunoblotting was performed using an anti-PLSCR1 antibody for PLSCR1 or an anti-actin antibody for actin. PCR was performed as follows: 20 cycles of amplification for G3PDH using HSTaq and 35 cycles of amplification for BMRF1 using KAPATaqEx. The intensities of the immunoblotted bands and the RT-PCR products were quantified using ImageJ, and the intensities of the products obtained using nontarget shRNA-transfected cells were defined as 1.0. *C*, C666-1 cells were transfected with 5 μg of a nontarget shRNA control or PLSCR1-specific shRNA. After 36 h of transfection, shRNA-transfected C666-1 cells were transfected with 1 μg of pcDNA3 or 3FG-BZLF1. After 48 h of the second transfection, total cell lysates were prepared. Total cell lysates (5 μg for BZLF1, PLSCR1, and actin and 15 μg for BMRF1) were subjected to SDS-PAGE, and immunoblotting was performed using an anti-FLAG M2 antibody for BZLF1, an anti-PLSCR1 for endogenous PLSCR1, an anti-actin antibody for endogenous actin, or an anti-BMRF1 antibody for endogenous BMRF1. The intensities of the immunoblotted bands were quantified using ImageJ, and the intensities of the products obtained using 3FG-BZLF1 and nontarget shRNA-transfected cells were defined as 1.0.

identical in the presence and absence of PLSCR1-specific shRNA (Fig. 6*C*, *lanes 3* and *4*, *second panel from the top*). Unfortunately, we were unable to detect endogenous BMRF1 protein expression, although the levels of BZLF1-induced BMRF1 protein were significantly increased in the PLSCR1-specific shRNA-transfected cells (Fig. 6*C*, *lanes 3* and *4*, *third panel from the top*). Taken together, these observations revealed that PLSCR1 represses BZLF1-dependent lytic gene expression in EBV-infected NPC cells.

PLSCR1 expression negatively regulates lytic gene expression in PLSCR1-KO EBV-infected NPC cells

To confirm the PLSCR1-mediated repression of BZLF1-dependent transactivation of lytic gene expression in PLSCR1-KO EBV-infected NPC cells, we generated the PLSCR1-KO C666-1 cells by using the CRISPR/Cas9 genome editing system. In contrast with parental C666-1 cells, PLSCR1 protein expression was barely detected in our PLSCR1-KO C666-1 cells (Fig. 7*A*, *top panel*). The results of semiquantitative RT-PCR assays demonstrated that the levels of G3PDH mRNA were almost identical in C666-1 and PLSCR1-KO C666-1 cells (Fig. 7*A*, *bottom panel*). However, the levels of BMRF1 mRNA increased approximately 2- to 4-fold in the PLSCR1-KO C666-1 cells compared with parental C666-1 cells (Fig. 7*A*, *third panel from top*).

Next, to examine whether the high levels of BMRF1 mRNA in PLSCR1-KO C666-1 cells were caused by the KO of the PLSCR1 gene, PLSCR1 was overexpressed in PLSCR1-KO C666-1 cells. The results of immunoblot analysis revealed that the epitope-tagged and untagged forms of PLSCR1 were efficiently expressed in cells transfected with 3M-PLSCR1 (Fig. 7*B*, *top panel*). The results of semiquantitative RT-PCR assays demonstrated that the levels of G3PDH mRNA in the 3M-PLSCR1–transfected cells were slightly lower than those observed in the empty vector–transfected cells (Fig. 6*B*, *middle panel*). However, the levels of BMRF1 mRNA were significantly decreased in the PLSCR1-overexpressed cells to ~40% of that observed in the empty vector–transfected cells. These results indicated that PLSCR expression decreased the levels of lytic BMRF1 mRNA in PLSCR1-KO C666-1 cells.

To confirm the PLSCR1-mediated repression of BZLF1-dependent transactivation at the protein level in PLSCR1-KO C666-1 cells, lytic BMRF1 protein expression was induced by transfecting cells with 3FG-BZLF1 in the presence or absence of 3M-PLSCR1. Consistent with previous observations, immunoblot analysis of the total cell lysates indicated that

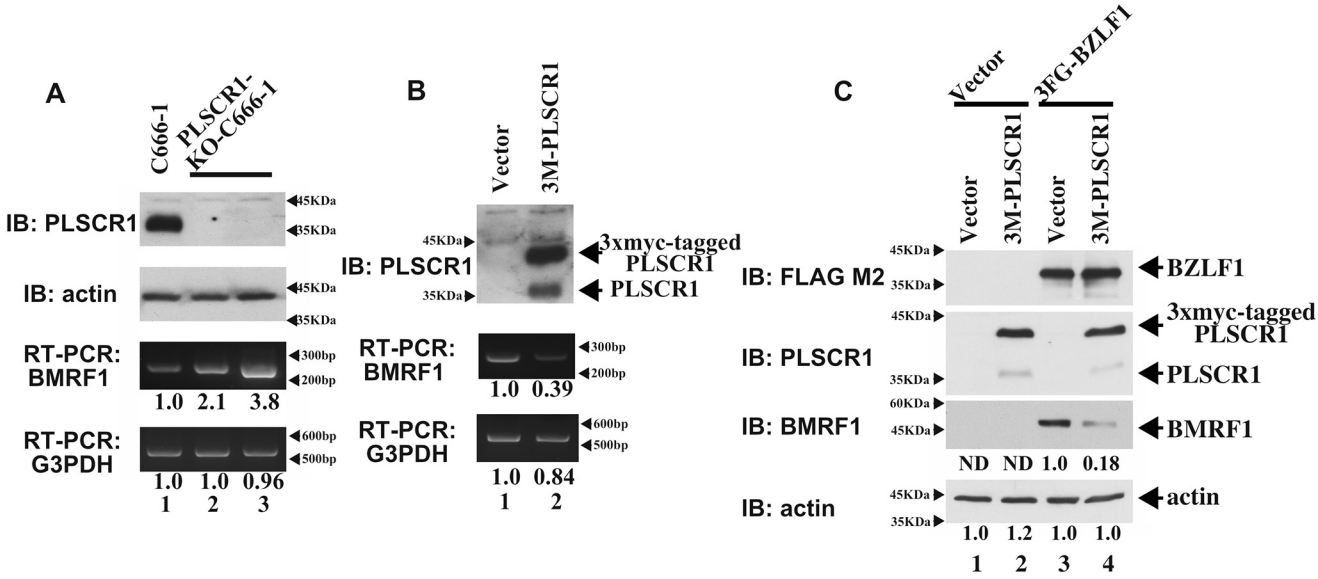

Figure 7. PLSCR1 expression decreases lytic BMRF1 mRNA and protein expression in PLSCR1-KO C666-1 cells. *A*, total cell lysates (10 μg) were subjected to SDS-PAGE, and immunoblotting was performed using an anti-PLSCR1 antibody for PLSCR1 or an anti-actin antibody for actin. PCR was performed as follows: 17 cycles of amplification for G3PDH using HSTaq and 27 cycles of amplification for BMRF1 using KAPATaqEx. Gel electrophoresis and quantification of RT-PCR products were performed as described in Fig. 6*A*. The levels of G3PDH or BMRF1 mRNA obtained from C666-1 cells were defined as 1.0. *B*, PLSCR1-KO C666-1 cells were transfected with 4 μg of pcDNA3 or 3M-PLSCR1. After 72 h of transfection, total cell lysates and total RNA were prepared. Total cell lysates (5 μg) were subjected to SDS-PAGE, and immunoblotting was performed using an anti-PLSCR1 antibody for PLSCR1. PCR was performed as follows: 20 cycles of amplification for G3PDH using HSTaq and 30 cycles of amplification for BMRF1 using KAPATaqEx. Gel electrophoresis and quantification of RT-PCR products were performed as described in Fig. 6*B*. The levels of G3PDH or BMRF1 mRNA obtained from empty vector–transfected cells were defined as 1.0. *C*, PLSCR1-KO C666-1 cells were transfected with 0.25 μg of pcDNA3 or 3FG-BZLF1 and 4 μg of pcDNA3 or 3M-PLSCR1. After 72 h of transfection, total cell lysates were prepared. Total cell lysates (5 μg for BZLF1, PLSCR1, and actin and 15 μg for BMRF1) were subjected to SDS-PAGE, and immunoblotting was performed using an anti–FLAG M2 antibody for BZLF1, an anti-PLSCR1 for endogenous PLSCR1, an anti-actin antibody for endogenous actin, or an anti-BMRF1 antibody for endogenous BMRF1. The intensities of the immunoblotted bands were quantified using ImageJ, and the intensities of the products obtained for the empty vector and 3FG-BZLF1–transfected cells were defined as 1.0.

3M-PLSCR1 transfection efficiently expressed the epitope-tagged and untagged forms of PLSCR1 (Fig. 7*C*, *lanes 2* and *4*, *second panel from the top*). The levels of BZLF1 expression were almost identical in the absence and presence of 3M-PLSCR1 (Fig. 7*C*, *lanes 3* and *4*, *top panel*), whereas the levels of BZLF1-induced BMRF1 protein were significantly decreased in the PLSCR1-overexpressed cells compared with the empty vector–transfected cells (Fig. 7*C*, *lanes 3* and *4*, *third panel from the top*). Taken together, these observations confirmed that PLSCR1 expression also represses BZLF1-dependent lytic gene expression in PLSCR1-KO EBV-infected NPC cells.

PLSCR1 decreases the levels of BZLF1-CBP complex

Because we previously reported that PLSCR1 represses the transactivation of HTLV-1 Tax by preventing its homodimerization (21) we next assessed whether PLSCR1 affects BZLF1 homodimerization. To minimize the effect of endogenous PLSCR1, HeLa-PLSKO cells stably expressing empty vector (HeLa-PLSKO-vector) or 3M-PLSCR1 (HeLa-PLSKO-3M-PLSCR1) were transfected with S epitope–tagged BZLF1 encoding amino acids 3–245 (S-BZLF1) and a 3×FLAG epitope–tagged bZIP motif of BZLF1 (3FG-BZLF1(160–245)). Immunoblot analysis of the total cell lysates revealed that all constructs were expressed at similar levels in the presence and absence of PLSCR1 (Fig. S2, *lanes 1–6*). Similarly, immunoblot analysis of the full-length BZLF1-precipitated complexes revealed that BZLF1(160–245) was co-precipitated with BZLF1 at similar levels in the presence and absence of PLSCR1 expression (Fig. S2, *lanes 8*, *9*, *11*, and *12*), indicating that PLSCR1 does not affect BZLF1 homodimerization.

For the efficient transactivation of EBV early promoters, BZLF1 interacts with the N-terminal region of the transcriptional co-activator CBP through its bZIP region (30). To determine whether PLSCR1 affects BZLF1-CBP complex formation, PLSCR1-KO HEK-293 cells were transfected with 3×FLAG epitope–tagged human CBP encoding amino acids 1–721 (3FG-CBP(1–721)), S-BZLF1, and 3M-PLSCR1. Immunoblot analysis of total cell lysates indicated that the expression levels of BZLF1 were almost identical, although slightly lower levels of CBP(1–721) were expressed in the absence of PLSCR1 among the S-BZLF1–transfected lysates (Fig. 8*A*, *lanes 3* and *4*). Interestingly, pulldown analysis using S-protein beads to precipitate BZLF1 revealed that PLSCR1 expression significantly decreased CBP(1–721) co-precipitation with BZLF1 (Fig. 8*A*, *lanes 7* and *8*).

To confirm this observation in other PLSCR1-KO cells, PLSCR1-KO HeLa cells stably expressing empty vector or 3M-PLSCR1 were transfected with 3FG-CBP(1–721) and S-BZLF1. Immunoblot analysis of the total cell lysates indicated that all constructs were expressed at similar levels in the presence and absence of PLSCR1 expression (Fig. 8*B*, *lanes 1–4*). However, pulldown analysis using S-protein beads to precipitate BZLF1 revealed that PLSCR1 expression significantly decreased CBP(1–721) co-precipitation with BZLF1 (Fig. 8*B*, *lanes 7* and *8*). These results revealed that PLSCR1 represses the interaction between BZLF1 and CBP *in vivo*.

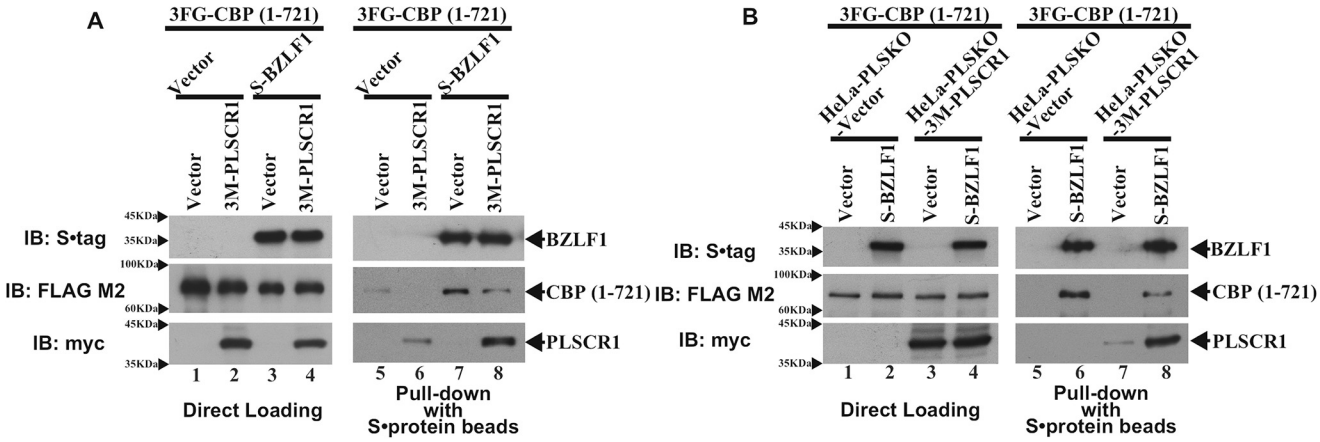

Figure 8. PLSCR1 decreases the levels of BZLF1·CBP complex. *A*, PLSCR1-KO HEK-293 cells were transfected with 1 μg of 3FG-CBP(1–721), 0.4 μg of pcDNA3 or S-BZLF1, and 3.6 μg of pcDNA3 or 3M-PLSCR1. A total of 500 μg of total cell lysate prepared using Nonidet P-40 lysis buffer, which was subsequently incubated with S-protein beads to precipitate BZLF1. Following pulldowns, 15 μg of total cell lysate and the precipitated complexes were divided into three portions and subjected to SDS-PAGE. Immunoblotting was performed using an anti–S-tag antibody for BZLF1, an anti–FLAG M2 antibody for CBP(1–721), or an anti-myc antibody for PLSCR1. *B*, PLSCR1-KO HeLa cells stably expressing empty vector or 3M-PLSCR1 were transfected with 1.6 μg of 3FG-CBP(1–721) and 0.8 μg of pcDNA3 or S-BZLF1. A total of 250 μg of total cell lysate prepared by using Nonidet P-40 lysis buffer was incubated with S-protein beads to precipitate BZLF1. Following pulldowns, 7.5 μg of total cell lysate and the precipitated complexes were divided into three portions and subjected to SDS-PAGE. Immunoblotting was performed using an anti–S-tag antibody for BZLF1, an anti–FLAG M2 antibody for CBP(1–721) or an anti-myc antibody for PLSCR1.

Discussion

This work reveals for the first time that PLSCR1 directly interacts with EBV BZLF1 *in vitro* and *in vivo* (Figs. 2 and 3) and that amino acids 1–163 and 160–250 of PLSCR1 (Fig. 2) and the C-terminal bZIP region of BZLF1 (Fig. 3) are involved in this interaction. Both BZLF1-binding regions of PLSCR1 contain an ID region (21) and interact with the ID regions of HTLV-1 Tax and HIV-1 Tat (21, 22). ID regions are known to confer conformational flexibility, which facilitates posttranslational modifications and enables a protein to functionally interact with many cellular partners (31). Interestingly, the bZIP region of BZLF1 exhibited more effective binding to PLSCR1 than did full-length BZLF1 (Fig. 3). These data are similar to the previous observation that the N-terminal 133 amino acid–truncated BZLF1 region more effectively interacts with the NF-κB p65 subunit than does the full-length molecule (32). Notably, DISPROT VSL2P analysis results indicated that the bZIP region of BZLF1 also contains a long ID region (169–216 amino acids) (33). This BZLF1 ID region may also alter its conformation so that it can interact with distinct regions of PLSCR1, and the N-terminal region of BZLF1 may affect the conformational change of the ID region of the bZIP region of BZLF1. The ID regions of both proteins likely play a key role in this protein-protein interaction.

Because BZLF1 plays a crucial role in the switch from latent to lytic EBV infection (8, 9), the functional consequences of the PLSCR1·BZLF1 interaction for BZLF1-dependent transactivation were assessed *in vivo*. Reporter analysis demonstrated that PLSCR1 overexpression effectively represses the BZLF1-dependent transactivation of the lytic BMRF1 promoter and that the BZLF1-binding regions of PLSCR1 are sufficient for this repression (Fig. 5). However, the N-terminal (1–163 amino acids)–binding region of PLSCR1 exhibited more effective repression than the 160–250-amino acid region (Fig. 5). Furthermore, in parental and PLSCR1-KO EBV-infected NPC cells, PLSCR1 overexpression decreased the expression of BZLF1 up-regulated lytic BMRF1 expression at the mRNA and protein levels, and the knockdown or KO of endogenous PLSCR1 expression increased the levels of BMRF1 mRNA (Figs. 6 and 7). However, we could not isolate virus particles from parental and PLSCR1-KO C666-1 cells, and we could not determine whether PLSCR1 expression also reduces virion production in EBV-infected NPC cells. Further investigation is warranted to confirm whether this elevated expression of PLSCR1 not only represses lytic gene expression but also reduces EBV virion production.

The interaction of BZLF1 with CBP through its dimerization domain is known to effectively enhance the BZLF1-mediated transactivation of early gene promoters (30). In this study, the results of pulldown assays revealed that PLSCR1 efficiently represses BZLF1-CBP complex formation in PLSCR1-KO HEK-293 and HeLa cells (Fig. 8). Notably, the PLSCR1-binding region of BZLF1 is included within the DNA-binding domain of the bZIP motif (Fig. 3). However, PLSCR1 competes with the C-terminal bZIP motif of BZLF1 for its interaction with CBP. Because the PLSCR1-binding region of BZLF1 is located next to the dimerization domain of BZLF1, PLSCR1 may sterically interfere with BZLF1-CBP complex formation. Furthermore, BZLF1 interacts with a number of host regulatory molecules, including the p53, NF-κB p65, and C/EBP proteins (32, 34, 35), and affects their functions. Further investigations are needed to determine whether PLSCR1 affects BZLF1-mediated regulation of host target molecules through protein-protein interactions in EBV-infected cells.

Although EBV can infect both B cells and epithelial cells, it typically establishes only latent infections in B cells. B-cell-specific transcription factors have been suggested to promote viral latency through the negative regulation of BZLF1 in B cells (6, 7). However, latent EBV infection occurs in EBV-associated epithelial malignancies, such as NPC and gastric cancers, and the negative regulatory mechanism(s) of BZLF1 may be involved in the development of EBV-associated epithelial

malignancies. The results of this study show for the first time that the basal expression of PLSCR1 was significantly elevated in EBV-infected NPC cells. (Fig. 1, *A* and *C*). However, the basal expression of PLSCR1 was significantly lower in EBV-infected BL cells, and IFN treatment strongly induced PLSCR1 expression these cells (Fig. 1*B*), consistent with our previous report on EBV-negative human epithelial cells (21). The precise induction mechanism of PLSCR1 expression in EBV-infected NPC cells remains unclear. Interestingly, the basal expression of PLSCR1 was also significantly elevated in the human epidermoid carcinoma cell line A431 in the absence of IFN (Fig. 1*A*). Because C666-1 and A431 cells originate from epidermal cells, we assessed the basal expression of PLSCR1 in EBV-negative human immortalized primary keratinocyte cells. Notably, the basal expression of PLSCR1 was also increased in two immortalized human epidermal keratinocyte cell lines, normal oral keratinocyte and HaCaT, similar to those observed in three EBV-infected NPC cells and an IFN-α–treated HeLa cell line (Fig. S3, *lanes 2–7*). The normal oral keratinocyte cell line is a human primary oral epithelial keratinocyte cell line immortalized by human telomerase, and the HaCaT cell line is a spontaneously immortalized human primary skin keratinocyte cell line. A previous report showed that human telomerase–immortalized primary keratinocytes exhibit similar properties to primary human keratinocytes (36). Thus, the basal expression of PLSCR1 may be elevated in human primary epidermal keratinocytes, similar to that in both immortalized human epidermal keratinocyte cell lines. This elevated expression of PLSCR1 in EBV-infected NPC cells may not arise from EBV infection but from these cells' epidermal origin. c-Myc has been suggested to up-regulate the expression of PLSCR1 by directly binding to its promoter in HEK-293 cells (37). c-Myc is also known to be predominantly expressed in the basal cell layers of the epidermis and is constitutively expressed in mouse primary keratinocytes (38, 39). This constitutive expression of c-Myc in the epidermis may play a key role for in high level of PLSCR1 expression in epidermal cells. However, further investigation is warranted to confirm whether the basal expression of PLSCR1 is significantly elevated in epidermal cells by using primary epidermal tissues and/or cells. Furthermore, EBV infection increases the expression of c-Myc through the STAT3 and NF-κB pathways in human nasopharyngeal epithelial cells (40), and c-Myc protein expression is negatively regulated in EBV latently infected type I and type III BL cells (41, 42). The levels of c-Myc protein may also play an important role in PLSCR1 expression in EBV-infected BL and NPC cells. Interestingly, IFN-α treatment has been shown to inhibit lytic gene expression in lytic replication–induced Daudi cells (43). The results of this study revealed that IFN-α treatment significantly induces PLSCR1 expression in EBV-positive BL cells, including Daudi cells (Fig. 1*B*). This IFN-α–induced high level of PLSCR1 expression may also contribute to the IFN-mediated repression of EBV lytic replication in EBV-infected BL cells through the negative regulation of BZLF1. Taken together, PLSCR1 expression may be enhanced by the EBV-dependent and -independent c-Myc up-regulation in EBV-infected NPC cells. Further investigation is warranted to determine whether c-Myc affects PLSCR1 expression in human epidermal cells. Furthermore, this high level of PLSCR1 expression may contribute to promoting viral latency through the negative regulation of BZLF1 by preventing BZLF1-CBP complex formation in EBV-infected NPC cells.

Experimental procedures

Materials

The EBV-infected NPC cell line C666-1 (44) and EBV-infected C15 and C17 NPC xenograft frozen tumors (45) were generously provided by N. Raab-Traub. A431, SW480, and MCF-7 cell lines were obtained from the Cell Resource Center for Biomedical Research, Cell Bank, Tohoku University. The anti-EBV EA-D-p52/50 (BMRF1) and histone H3 (96C10) antibodies used in this study were purchased from Chemicon and Cell Signaling Technology, respectively. Immunoblotting, cDNA preparation, PCR amplification for cloning, and sequencing of all DNA constructs were performed as described previously (46, 47). Other materials used in this study were obtained as described previously (21).

Plasmid construction

PLSCR1 and its mutant expression plasmids were constructed as described previously (21). BZLF1 cDNA encoding amino acids 3–245 was PCR amplified from EBV-infected NPC cell line C666-1 cDNA and cloned into pcDNA3 (Invitrogen), and 3×FLAG or S epitopes were added at the N terminus to produce 3FG-BZLF1 and S-BZLF1, respectively. BZLF1 mutant cDNA fragments encoding amino acids 28–245, 86–245, 3–227, 3–196, 3–169, and 160–245 were PCR amplified from 3FG-BZLF1 and cloned into pcDNA3 with a 3×FLAG epitope at the N terminus to produce 3FG-BZLF1(28–245), 3FG-BZLF1(86–245), 3FG-BZLF1(3–227), 3FG-BZLF1(3–196), 3FG-BZLF1(3–169), and 3FG-BZLF1(160–245), respectively. Full-length PLSCR1 tagged with three myc epitopes was PCR amplified from 3M-PLSCR1 (21) and cloned into pIRESpuro3 (Clontech) to produce pIRp3–3M-PLSCR1. Human CBP cDNA encoding amino acids 1–721 was PCR amplified from C666-1 cDNA and cloned into pcDNA3, with a 3×FLAG epitope added at the N terminus to produce 3FG-CBP (1–721). The EBV lytic BMRF1 promoter sequence was PCR amplified from C666-1 genomic DNA using the primers 5′-cggatccGACGCTGGCGAGCCGGGCCG-3′ and 5′-caagatctGTACGTGATGAAACAGGCAA-3′ and was subsequently cloned into pGL4.10 (Promega) to produce pBMRF1pro-4.10.

Bacterial protein expression and pulldown assays

Bacterial protein expression and pulldown assays were performed as described previously (21)

Cell culture and transfection

HEK-293, COS-1, HeLa, A431, and MCF-7 cells were maintained in Dulbecco's modified Eagle's medium (DMEM) supplemented with penicillin and streptomycin (PS) (Biological Industries) and 10% fetal bovine serum (FBS) (Gibco BRL) as described previously (21, 48). SW480 cells were maintained DMEM/F-12 medium containing PS and 10% FBS. C666-1, BJAB, B95–8, Namalwa, P3HR1, and Daudi cells were main-

tained in RPMI 1640 medium containing PS and 10% FBS. For pulldown and immunoprecipitation assays, HEK-293 and PLSCR1-KO HEK-293 cells (1×10^6) were plated in 60-mm cell culture plates and were transfected with the indicated amounts of DNA using jetPEI (Polyplus Transfection) as suggested by the manufacturer. For the luciferase assay and immunofluorescence analysis, COS-1 cells were transfected with the indicated amounts of DNA using jetPEI or TransIT-LT1 (Mirus) as suggested by the manufacturer. HeLa and PLSCR1-KO HeLa cells (5×10^5) were plated in 60-mm cell culture plates and transfected with the indicated amounts of DNA using jetPRIME (Polyplus Transfection) as suggested by the manufacturer. C666-1 and PLSCR1-KO C666-1 cells (9×10^5) were plated in fibronectin-coated 60-mm cell culture plates and were transfected with the indicated amounts of DNA using TransIT-X2 Dynamic Delivery System (Mirus) as suggested by the manufacturer.

CRISPR/Cas9 plasmid construction and PLSCR1 gene KO

For Cas9-mediated editing of the PLSCR1 gene, the targeting 20-mer for the guided RNA (in exon 2: 5′-CGGAAACAAACTTGCCAGTT-3′) was cloned into the plasmid pJWB1157 (generously provided by E. Johannsen and M. Ohashi), which is derived from pX330 (48). The Cas9 expression cassette and guided RNA were excised from pJWB1157 using the restriction enzymes PciI and NotI and were cloned into pCEP4 with a modified polylinker sequence (pCEP4-CRISPR) (generously provided by E. Johannsen and M. Ohashi), which allowed for hygromycin selection through a self-maintaining episomal plasmid (48), generating pCEP-CRISPR-PLSCR1. HEK-293, HeLa, and C666-1 cells were transfected with 5 μg of pCEP-CRISPR-PLSCR1 as described previously. Next, 48 h after transfection, the HEK-293, HeLa, and C666-1 cells were selected with 250, 400, and 20 μg/ml of hygromycin B (Nacalai Tesque) for 2 weeks, respectively. Hygromycin-resistant cells were harvested and screened via immunoblot analyses in the presence of IFN-α. Subsequently, the knockdown of the PLSCR1 gene was confirmed by Sanger sequencing of PCR products amplified using a set of primers (5′-CTCTGAGAACAGGCACAGCT-3′ and 5′-AAGAACAACTAGGCTGCCAAAA-3′).

Preparation of empty vector or stable PLSCR1-expressing PLSCR1-KO HeLa cells

PLSCR1-KO HeLa cells were transfected with empty vector (pIRES-puro3) or pIRp3–3M-PLSCR1 as described previously. Next, 48 h after transfection, the PLSCR1-KO HeLa cells were selected with 2 μg/ml of puromycin (InvivoGen) for 2 weeks. Subsequently, puromycin-resistant cells were harvested and 3×myc epitope–tagged PLSCR1 expression was confirmed by immunoblot analyses using an anti-myc antibody.

Pulldown and immunoprecipitation assays using transfected cell lysates

Forty-eight h after transfection, cells were harvested and lysed in CHAPS lysis buffer (47) or Nonidet P-40 lysis buffer (25 mM Tris-HCl, pH 7.5, 150 mM sodium chloride, 0.1% Nonidet P-40 (Nacalai Tesque), and 10% glycerol) containing a protease inhibitor mixture (Sigma). Pulldown and immunoprecipitation were performed using S-protein agarose beads (Novagen) and anti-FLAG M2 beads (Sigma) to precipitate the S epitope–tagged and 3×FLAG epitope–tagged proteins, respectively, as previously described (21).

Immunofluorescence analysis

Immunofluorescence analysis was performed as described previously (46).

Subcellular fractionation

The subcellular fractionation was performed as described previously (21).

Dual luciferase assay

Dual luciferase assays were performed as described previously (46).

Semiquantitative RT-PCR

Total cell lysates and total RNA were prepared as described previously (47). First-strand cDNA was synthesized from 0.5 μg of total RNA from each sample as described previously (49). PCR was performed using 1 μl of a 4-fold dilution of each cDNA reaction mix and primer sets for human G3PDH (47) and BMRF1 (5′-CTAGCCGTCCTGTCCAAGTGC-3′ and 5′-AGCCAAACAGCTCCTTGCCCA-3′) (50). PCR was performed using the indicated DNA polymerases for the indicated number of amplification cycles, as suggested by the manufacturer. PCR products were subjected to agarose gel electrophoresis, and DNA bands were visualized using Gel Green Nucleic Acid Gel Stain (Biotium).

Author contributions—S. K. funding acquisition; S. K. investigation; S. K. methodology; S. K. writing-original draft; S. K. project administration; M. I. supervision; M. I. writing-review and editing.

Acknowledgments—We thank N. Raab-Traub (University of North Carolina, Chapel Hill) for providing the C666-1 cells, and the C15 and C17 NPC tumors; the Cell Resource Center for Biomedical Research, Cell Bank (Tohoku University) for providing the A431, SW480, and MCF-7 cells; as well as E. Johannsen and M. Ohashi (University of Wisconsin, Madison) for the pJWB1157 and pCEP4-CRISPR plasmids.

References

1. Raab-Traub, N. (1996) Pathogenesis of Epstein-Barr virus and its associated malignancies. *Semin. Virol.* **7,** 315–323 CrossRef
2. Tsao, S. W., Tsang, C. M., Pang, P. S., Zhang, G., Chen, H., and Lo, K. W. (2012) The biology of EBV infection in human epithelial cells. *Semin. Cancer Biol.* **22,** 137–143 CrossRef Medline
3. Kieff, E., and Rickinson, A. B. (2001) Epstein-Barr Virus and Its Replication. In *Fields Virology* (Fields, B., Knipe, D., and Howley, P., eds) 4th Ed., pp. 2511–2573, Lippincott-Raven Publishers, Philadelphia PA
4. Rickinson, A. B., and Kieff, E. (2001) Epstein-Barr Virus. In *Fields Virology*(Fields, B., Knipe, D., and Howley, P., eds.) 4th Ed., pp. 2575–2627, Lippincott-Raven Publishers, Philadelphia PA
5. Raab-Traub, N. (2002) Epstein-Barr virus in the pathogenesis of NPC. *Semin. Cancer Biol.* **12,** 431–441 CrossRef Medline
6. Robinson, A. R., Kwek, S. S., and Kenney, S. C. (2012) The B-cell specific transcription factor, Oct-2, promotes Epstein-Barr virus latency by inhib-

iting the viral immediate-early protein, BZLF1. *PLoS Pathog.* **8,** e1002516 CrossRef Medline
7. Raver, R. M., Panfil, A. R., Hagemeier, S. R., and Kenney, S. C. (2013) The B-cell-specific transcription factor and master regulator Pax5 promotes Epstein-Barr virus latency by negatively regulating the viral immediate early protein BZLF1. *J. Virol.* **87,** 8053–8063 CrossRef Medline
8. Tsurumi, T., Fujita, M., and Kudoh, A. (2005) Latent and lytic Epstein-Barr virus replication strategies. *Rev. Med. Virol.* **15,** 3–15 CrossRef Medline
9. Chen, C., Li, D., and Guo, N. (2009) Regulation of cellular and viral protein expression by the Epstein-Barr virus transcriptional regulator Zta: Implications for therapy of EBV associated tumors. *Cancer Biol. Ther.* **8,** 987–995 CrossRef Medline
10. Lieberman, P. M., Hardwick, J. M., Sample, J., Hayward, G. S., and Hayward, S. D. (1990) The zta transactivator involved in induction of lytic cycle gene expression in Epstein-Barr virus-infected lymphocytes binds to both AP-1 and ZRE sites in target promoter and enhancer regions. *J. Virol.* **64,** 1143–1155 Medline
11. Sinclair, A. J. (2003) bZIP proteins of human gammaherpesviruses. *J. Gen. Virol.* **84,** 1941–1949 CrossRef Medline
12. Zhou, Q., Zhao, J., Stout, J. G., Luhm, R. A., Wiedmer, T., and Sims, P. J. (1997) Molecular cloning of human plasma membrane phospholipid scramblase. A protein mediating transbilayer movement of plasma membrane phospholipids. *J. Biol. Chem.* **272,** 18240–18244 CrossRef Medline
13. Suzuki, J., Umeda, M., Sims, P. J., and Nagata, S. (2010) Calcium-dependent phospholipid scrambling by TMEM16F. *Nature* **468,** 834–838 CrossRef Medline
14. Bevers, E. M., and Williamson, P. L. (2010) Phospholipid scramblase: An update. *FEBS Lett.* **584,** 2724–2730 CrossRef Medline
15. Yu, A., McMaster, C. R., Byers, D. M., Ridgway, N. D., and Cook, H. W. (2003) Stimulation of phosphatidylserine biosynthesis and facilitation of UV-induced apoptosis in Chinese hamster ovary cells overexpressing phospholipid scramblase 1. *J. Biol. Chem.* **278,** 9706–9714 CrossRef Medline
16. Li, Y., Rogulski, K., Zhou, Q., Sims, P. J., and Prochownik, E. V. (2006) The negative c-Myc target onzin affects proliferation and apoptosis via its obligate interaction with phospholipid scramblase 1. *Mol. Cell. Biol.* **26,** 3401–3413 CrossRef Medline
17. Der, S. D., Zhou, A., Williams, B. R., and Silverman, R. H. (1998) Identification of genes differentially regulated by interferon α, β, or γ using oligonucleotide arrays. *Proc. Natl. Acad. Sci. U.S.A.* **95,** 15623–15628 CrossRef Medline
18. Dong, B., Zhou, Q., Zhao, J., Zhou, A., Harty, R. N., Bose, S., Banerjee, A., Slee, R., Guenther, J., Williams, B. R., Wiedmer, T., Sims, P. J., and Silverman, R. H. (2004) Phospholipid scramblase 1 potentiates the antiviral activity of interferon. *J. Virol.* **78,** 8983–8993 CrossRef Medline
19. Zhao, K. W., Li, D., Zhao, Q., Huang, Y., Silverman, R. H., Sims, P. J., and Chen, G. Q. (2005) Interferon-α-induced expression of phospholipid scramblase 1 through STAT1 requires the sequential activation of protein kinase Cδ and JNK. *J. Biol. Chem.* **280,** 42707–42714 CrossRef Medline
20. Thornburg, N. J., Kusano, S., and Raab-Traub, N. (2004) Identification of Epstein-Barr virus RK-BARF0-interacting proteins and characterization of expression pattern. *J. Virol.* **78,** 12848–12856 CrossRef Medline
21. Kusano, S., and Eizuru, Y. (2012) Human phospholipid scramblase 1 interacts with and regulates transactivation of HTLV-1 Tax. *Virology* **432,** 343–352 CrossRef Medline
22. Kusano, S., and Eizuru, Y. (2013) Interaction of the phospholipid scramblase 1 with HIV-1 Tat results in the repression of Tat-dependent transcription. *Biochem. Biophys. Res. Commun.* **433,** 438–444 CrossRef Medline
23. Luo, W., Zhang, J., Liang, L., Wang, G., Li, Q., Zhu, P., Zhou, Y., Li, J., Zhao, Y., Sun, N., Huang, S., Zhou, C., Chang, Y., Cui, P., Chen, P., *et al.* (2018) Phospholipid scramblase 1 interacts with influenza A virus NP, impairing its nuclear import and thereby suppressing virus replication. *PLoS Pathog.* **14,** e1006851 CrossRef Medline
24. Frasch, S. C., Henson, P. M., Nagaosa, K., Fessler, M. B., Borregaard, N., and Bratton, D. L. (2004) Phospholipid flip-flop and phospholipid scramblase 1 (PLSCR1) co-localize to uropod rafts in formylated Met-Leu-Phe-stimulated neutrophils. *J. Biol. Chem.* **279,** 17625–17633 CrossRef Medline
25. Yuan, Y., Tian, C., Gong, Q., Shang, L., Zhang, Y., Jin, C., He, F., and Wang, J. (2015) Interactome map reveals phospholipid scramblase 1 as a novel regulator of hepatitis B virus X protein. *J. Proteome Res.* **14,** 154–163 CrossRef Medline
26. Talukder, A. H., Bao, M., Kim, T. W., Facchinetti, V., Hanabuchi, S., Bover, L., Zal, T., and Liu, Y. J. (2012) Phospholipid scramblase 1 regulates Toll-like receptor 9-mediated type I interferon production in plasmacytoid dendritic cells. *Cell Res.* **22,** 1129–1139 CrossRef Medline
27. Hicks, M. R., Balesaria, S., Medina-Palazon, C., Pandya, M. J., Woolfson, D. N., and Sinclair, A. J. (2001) Biophysical analysis of natural variants of the multimerization region of Epstein-Barr virus lytic-switch protein BZLF1. *J. Virol.* **75,** 5381–5384 CrossRef Medline
28. Wiedmer, T., Zhao, J., Nanjundan, M., and Sims, P. J. (2003) Palmitoylation of phospholipid scramblase 1 controls its distribution between nucleus and plasma membrane. *Biochemistry* **42,** 1227–1233 CrossRef Medline
29. Flemington, E. K., Borras, A. M., Lytle, J. P., and Speck, S. H. (1992) Characterization of the Epstein-Barr virus BZLF1 protein transactivation domain. *J. Virol.* **66,** 922–929 Medline
30. Adamson, A. L., and Kenney, S. (1999) The Epstein-Barr virus BZLF1 protein interacts physically and functionally with the histone acetylase CREB-binding protein. *J. Virol.* **73,** 6551–6558 Medline
31. Radivojac, P., Iakoucheva, L. M., Oldfield, C. J., Obradovic, Z., Uversky, V. N., and Dunker, A. K. (2007) Intrinsic disorder and functional proteomics. *Biophys. J.* **92,** 1439–1456 CrossRef Medline
32. Gutsch, D. E., Holley-Guthrie, E. A., Zhang, Q., Stein, B., Blanar, M. A., Baldwin, A. S., and Kenney, S. C. (1994) The bZIP transactivator of Epstein-Barr virus, BZLF1, functionally and physically interacts with the p65 subunit of NF-kappa B. *Mol. Cell. Biol.* **14,** 1939–1948 CrossRef Medline
33. Peng, K., Radivojac, P., Vucetic, S., Dunker, A. K., and Obradovic, Z. (2006) Length-dependent prediction of protein intrinsic disorder. *BMC Bioinformatics* **7,** 208 CrossRef Medline
34. Zhang, Q., Gutsch, D., and Kenney, S. (1994) Functional and physical interaction between p53 and BZLF1: Implications for Epstein-Barr virus latency. *Mol. Cell. Biol.* **14,** 1929–1938 CrossRef Medline
35. Bristol, J. A., Robinson, A. R., Barlow, E. A., and Kenney, S. C. (2010) The Epstein-Barr virus BZLF1 protein inhibits tumor necrosis factor receptor 1 expression through effects on cellular C/EBP proteins. *J. Virol.* **84,** 12362–12374 CrossRef Medline
36. Smits, J. P. H., Niehues, H., Rikken, G., van Vlijmen-Willems, I. M. J. J., van de Zande G. W. H. J. F, Zeeuwen, P. L. J. M., Schalkwijk, J., and van den Bogaard, E. H. (2017) Immortalized N/TERT keratinocytes as an alternative cell source in 3D human epidermal models. *Sci. Rep.* **7,** 11838 CrossRef Medline
37. Vinnakota, J. M., and Gummadi, S. N. (2016) Two c-Myc binding sites are crucial in upregulating the expression of human phospholipid scramblase 1 gene. *Biochem. Biophys. Res. Commun.* **469,** 412–417 CrossRef Medline
38. Dotto, G. P., Gilman, M. Z., Maruyama, M., and Weinberg, R. A. (1986) c-myc and c-fos expression in differentiating mouse primary keratinocytes. *EMBO J.* **5,** 2853–2857 CrossRef Medline
39. Watt, F. M., Frye, M., and Benitah, S. A. (2008) MYC in mammalian epidermis: How can an oncogene stimulate differentiation. *Nat. Rev. Cancer* **8,** 234–242 CrossRef Medline
40. Lo, A. K., Lo, K. W., Tsao, S. W., Wong, H. L., Hui, J. W., To, K. F., Hayward, D. S., Chui, Y. L., Lau, Y. L., Takada, K., and Huang, D. P. (2006) Epstein-Barr virus infection alters cellular signal cascades in human nasopharyngeal epithelial cells. *Neoplasia* **8,** 173–180 CrossRef Medline
41. Ruf, I. K., Rhyne, P. W., Yang, H., Borza, C. M., Hutt-Fletcher, L. M., Cleveland, J. L., and Sample, J. T. (1999) Epstein-Barr virus regulates

c-MYC, apoptosis, and tumorigenicity in Burkitt lymphoma. *Mol. Cell. Biol.* **19,** 1651–1660 CrossRef Medline

42. Cooper, A., Johannsen, E., Maruo, S., Cahir-McFarland, E., Illanes, D., Davidson, D., and Kieff, E. (2003) EBNA3A association with RBP-Jκ down-regulates c-*myc* and Epstein-Barr virus-transformed lymphoblast growth. *J. Virol.* **77,** 999–1010 CrossRef Medline
43. Sharp, N. A., Arrand, J. R., and Clemens, M. J. (1989) Epstein-Barr virus replication in interferon-treated cells. *J. Gen. Virol.* **70,** 2521–2526 CrossRef Medline
44. Shair, K. H., Schnegg, C. I., and Raab-Traub, N. (2008) EBV latent membrane protein 1 effects on plakoglobin, cell growth, and migration. *Cancer Res.* **68,** 6997–7005 CrossRef Medline
45. Morrison, J. A., Gulley, M. L., Pathmanathan, R., and Raab-Traub, N. (2004) Differential signaling pathways are activated in the Epstein-Barr virus-associated malignancies nasopharyngeal carcinoma and Hodgkin lymphoma. *Cancer Res.* **64,** 5251–5260 CrossRef Medline
46. Kusano, S., and Eizuru, Y. (2010) Human I-mfa domain proteins specifically interact with KSHV LANA and affect its regulation of Wnt signaling-dependent transcription. *Biochem. Biophys. Res. Commun.* **396,** 608–613 CrossRef Medline
47. Kusano, S., Shiimura, Y., and Eizuru, Y. (2011) I-mfa domain proteins specifically interact with SERTA domain proteins and repress their transactivating functions. *Biochimie* **93,** 1555–1564 CrossRef Medline
48. Ohashi, M., Holthaus, A. M., Calderwood, M. A., Lai, C. Y., Krastins, B., Sarracino, D., and Johannsen, E. (2015) The EBNA3 family of Epstein-Barr virus nuclear proteins associates with the USP46/USP12 deubiquitination complexes to regulate lymphoblastoid cell line growth. *PLoS Pathog.* **11,** e1004822 CrossRef Medline
49. Kusano, S., Yoshimitsu, M., Hachiman, M., and Ikeda, M. (2015) I-mfa domain proteins specifically interact with HTLV-1 Tax and repress its transactivating functions. *Virology* **486,** 219–227 CrossRef Medline
50. Wen, W., Iwakiri, D., Yamamoto, K., Maruo, S., Kanda, T., and Takada, K. (2007) Epstein-Barr virus BZLF1 gene, a switch from latency to lytic infection, is expressed as an immediate-early gene after primary infection of B lymphocytes. *J. Virol.* **81,** 1037–1042 CrossRef Medline